Macromolecules

ARTICLE

pubs.acs.org/Macromolecules

Method To Measure the Viscoelastic Properties of Nanometer Entangled Polymer Films

Dongdong Peng, Zhaohui Yang,† and Ophelia K. C. Tsui*

Department of Physics, Boston University, Boston, Massachusetts 02215, United States

ABSTRACT: In this paper, we report a method to measure the viscoelastic properties, namely the plateau shear modulus and zero-shear viscosity, of nanometer polymer films. In this method, atomic force microscopy (AFM) is used to capture the surface topographic image of the films at different times as they are annealed at the measurement temperature. A model is developed based on the dynamics of surface capillary waves to analyze the data. We demonstrate how this method was applied to measure the viscoelastic properties of polystyrene films supported by silicon with thicknesses of 3 and 125 nm.

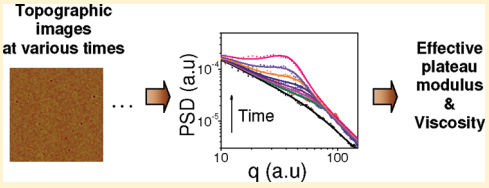

INTRODUCTION

Thin polymer films have widespread applications, including surface coating, microelectronics, biomedical engineering, etc. There has been mounting evidence over the past two decades showing that the glass transition temperature T_g of thin polymer films with thickness in the nanometer range can be significantly different from the bulk T_g.[1−5] As the temperature of a polymer is increased past the T_g, the polymer transforms from the solidlike glassy state to the liquid state. So the observed variation in the T_g can imply that the thermomechanical stability of a polymer nanoobject can be very different from its bulk counterpart,[6] raising issues concerning the use of polymers in nanoscale applications. Numerous experiments have been carried out to determine the change, if any, in the temperature-dependent dynamic properties of thin polymer films.[7−19] However, the results have so far been inconclusive. One possible reason is that the dynamics of thin polymer films may not follow the time−temperature superposition principle well-known for polymers.[9,18] As a result, thin polymer films may exhibit dynamic behavior that agrees with the bulk polymer at one temperature but not at another. To clarify if the thermomechanical stability of thin polymer films may be different from the bulk, it is therefore necessary to measure their dynamo-mechanical properties near the T_g directly. However, measurements of this sort are rare, especially for films with thickness below ∼10 nm.[5] Recently, we have developed a method to measure the viscosity of polymer films with thickness down to 2.3 nm for temperatures covering more than ±30 °C about the bulk T_g.[17,18] However, that method was only applicable to unentangled polymer films or films that are purely viscous. On the other hand, the majority of polymers used in practice are entangled and viscoelastic, so a different method is required. In this paper, we describe a method by which we were able to measure the effective plateau shear modulus and zero-shear viscosity of entangled polymer films with thickness down to 3 nm. Similar to the previous method,[17] the present method is also based on the use of atomic force microscopy (AFM) to monitor the evolution of the topographic fluctuations of the films as they dewet upon annealing. The main difference is that we have adapted a model analysis suitable for viscoelastic films.

EXPERIMENTAL SECTION

The polymers used are polystyrene (PS) homopolymers, purchased from Scientific Polymer Products, Inc. (Ontario, NY), with molecular weights (M_w) of 115 and 212 kg/mol (cf. the entanglement M_w of PS is ∼20 kg/mol) and polydispersity index of 1.08. Solutions of the polymers in toluene were spun-cast onto substrates made of ∼1 × ∼1 cm^2 silicon (100) wafers covered by a 100 ± 5 nm thick SiO_x layer to produce thin films that are 3 and 125 nm thick. Before spin-coating, the substrates were cleaned in a piranha solution (i.e., a mixture of H_2SO_4 and H_2O_2 in 7:3 by volume) at 130 °C for 20 min and then thoroughly rinsed in deionized water and dried in pure nitrogen gas before exposed to oxygen plasma for 20 min. The polymer thickness was controlled by varying the solution concentration and spin-coating speed and measured by ellipsometry with typically reproducibility of ±0.2 nm at different film locations. Previous studies[20−23] showed that these films dewetted when they were heated above their T_g. We quantify the initial roughening process, well before any holes are formed, by measuring the surface topographic image of the films with tapping-mode AFM at different annealing times at a given elevated temperature, T.[17,18,20,24,25] Most of the measurements were carried out *ex situ*, with the films being quenched to room temperature before imaging by AFM. We found no detectable difference in the result when we performed the measurements *in situ*. To prepare the data for analysis, we multiplied each AFM topographic image by a Welch function before Fourier transforming it to produce the 2-dimensional Fourier spectrum. Then we radial averaged the Fourier spectrum to obtain the power spectral density (PSD).[20] Below we describe the model analysis we use to analyze the PSDs in extracting the viscoelastic properties of the films.

THEORETICAL BACKGROUND

In our previous work,[18,24] we showed that the early stage (where the film roughness is $\ll h$) temporal (t) evolution of the

Received: June 6, 2011
Revised: August 8, 2011
Published: August 19, 2011

PSD of thin polymer films ($A_q^2(t)$) annealed at temperature, T, can be described by

$$A_q^2(t) = A_q^2(0)\exp(2\omega_q t) + \left[\frac{k_B T}{G''(h) + \gamma q^2}\right](1 - \exp(2\omega_q t)) \quad (1)$$

Here, k_B is the Boltzmann constant, ω_q is the relaxation rate of the surface capillary mode with wavevector q, and $G(h)$ and γ are respectively the van der Waals (vdW) potential[26] and surface tension of the film. Safran et al. had derived an expression for ω_q for viscoelastic films by solving the Laplace transform of the Navier−Stokes equation in the lubrication approximation:[27]

$$\omega_q = -\frac{h^3}{3\eta(\omega)}[G''(h)q^2 + \gamma q^4] \quad (2)$$

where h is the film thickness and $\eta(\omega)$ is the frequency-dependent viscosity appropriate for the Laplace formulation.[27] For simple viscous liquid films, $\eta(\omega)$ is a constant. With this, eq 2 recovers the expression for ω_{liq}, i.e., the relaxation rate for surface capillary modes for simple liquid films.[18] For viscoelastic films that exhibit elastic behavior at short times (characterized by shear modulus, $\mu_{plateau}$), but viscous behavior (with viscosity, $\eta \equiv \mu_{plateau}\tau_r$) after a characteristic relaxation time, τ_r, the dynamo-mechanical behavior is describable by the Maxwell liquid model[28] for which $\eta(\omega) = \mu_{plateau}/(\omega + \omega_r)$, where $\omega_r \equiv 1/\tau_r$.[27] In this study, we use the Maxwell model to simulate the dynamic behavior of entangled polymers that are initially in the rubbery plateau regime (with plateau modulus, $\mu_{plateau}$) but transition to the terminal flow regime (with viscosity, $\eta \equiv \mu_{plateau}\tau_r$) after the reptation time, τ_r. We note that the Maxwell model, assuming a single relaxation time, can be oversimplified for polymer films, whose dynamics are broadly perceived to be heterogeneous, with the near-surface region being more mobile, the middle region being the same as, and the substrate region being less mobile than the bulk.[3,7,18,29] Despite this heterogeneity, one may still expect the stress relaxation modulus of the films to decay to zero in a nearly exponential manner on time scales longer than the longest relaxation time.[28] In that case, the relation $\eta \equiv \mu(\tau_r)\tau_r$[28] should hold and the Maxwell model may be adequate. We shall see below that the Maxwell model indeed provides a reasonably good description to the data, which attests to its applicability. It should also be noted that the present model assumes the films to be homogeneous so that η and $\mu_{plateau}$ are both constant parameters, independent of position. It should thus be understood that the values of η and $\mu_{plateau}$ deduced here are effective (or average) values. It is also important to point out that the AFM does not act as a surface viscoelasticity probe here as it did in most other AFM thin film studies,[10,11,30−33] where the film surface was actively perturbed by a nanometer probe tip to induce a mechanical response. Instead, the AFM in this experiment passively maps the surface topography of the films arising from thermal excitation of the surface capillary modes. As a result, our measurements would not weigh the surface viscoelastic properties of the films more heavily than that predicted by the surface capillary wave theory. In a previous study,[18] we had demonstrated how in the context of the surface capillary wave theory the surface viscosity, if different from that of the film body, may affect the effective viscosity of purely viscous films and whereby the dynamic heterogeneity of the films can be deduced.

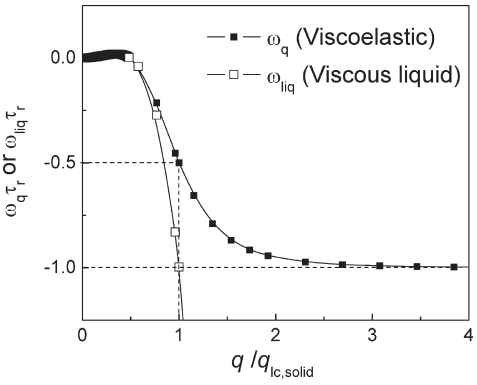

Figure 1. Surface capillary relaxation rates (ω_q and ω_{liq}) normalized by $1/\tau_r$ plotted versus the wavevector normalized by the elastic-state lower cutoff wavevector, $q_{lc,solid}$. The solid squares denote the plot of ω_q as given by eq 3, appropriate for viscoelastic films. The open squares denote the plot of ω_{liq}, appropriate for viscous liquid films. The vertical dashed line shows where $q/q_{lc,solid} = 1$. The horizontal dashed lines highlight the facts that $\omega(q_{lc,solid})\tau_r = -0.5$ and $\omega_{liq}(q_{lc,solid})\tau_r = -1$.

In this paper, we focus on how the effective viscosity and plateau modulus of viscoelastic polymer films can be determined in the first place. The question of how to determine the dynamic heterogeneity in these films will be the subject of a future publication.

By substituting the above expression of $\eta(\omega)$ in eq 2, we obtain

$$\omega_q = \frac{-\frac{h^3}{3}q^2(\gamma q^2 + G'')\omega_r}{\mu_{plateau} + \frac{h^3}{3}q^2(\gamma q^2 + G'')} = \frac{\omega_{liq}}{1 - \omega_{liq}\tau_r} \quad (3)$$

where $\omega_{liq} = -(h^3/3\eta)[G''(h)q^2 + \gamma q^4]$. By eq 3, ω_q is $\approx\omega_{liq}$ when $|\omega_{liq}\tau_r| \ll 1$ but $\approx -1/\tau_r$ when $|\omega_{liq}\tau_r| \gg 1$. At the crossover where $\omega_{liq}\tau_r = -1$, $\omega_q\tau_r = \omega_{liq}\tau_r/2$. We neglect the case where $\omega_{liq}\tau_r = 1$, which we will justify shortly. The condition for the crossover just mentioned, $\omega_{liq}\tau_r = -1$ can be shown to be equivalent to

$$\gamma q^2 + G'' = \frac{3\mu_{plateau}}{h^3 q^2} \quad (4)$$

and is fulfilled when $q = q_{lc,solid}$, the lower cutoff wavevector[25] of the theoretical PSD of elastic films with shear modulus $\mu_{plateau}$, thickness h, and vdW potential, G''. Figure 1 shows plots of $\omega_q\tau_r$ (as given by eq 3) (solid squares) and $\omega_{liq}\tau_r$ (open squares) versus $q/q_{lc,solid}$. As seen, ω_q and ω_{liq} can both be positive or negative depending on the value of q. Negative ω_q or ω_{liq} means that the films are stable while positive values mean otherwise.[27] From eq 3, we can see that instability occurs at small q's less than the critical value, $q_c = (-G''/\gamma)^{1/2}$ provided $(1 - \omega_{liq}\tau_r) > 0$. (Notice that G'' is always negative for the films studied here.[26]) The condition $(1 - \omega_{liq}\tau_r) > 0$ is equivalent to

$$\mu_{plateau} > -h^3 q^2(\gamma q^2 + G'')/3 \quad (5)$$

We notice that the upper limit of $-h^3q^2(\gamma q^2 + G'')/3$ occurs when $q = q_c/\sqrt{2}$ whereat it is equal to $\gamma h^3 q_c^4/12 = h^3 G''^2/(12\gamma)$. Because $|G''|$ decreases monotonically with increasing h for $h < \sim$200 nm,[20,26] which is the range of h we are interested in, the right-hand side of eq 5 is bigger for smaller h. In this experiment, the smallest h used was >2 nm. By using $G''(h) \approx 9 \times 10^{13}$ J/m^4

dx.doi.org/10.1021/ma201279c |Macromolecules 2011, 44, 7460–7464

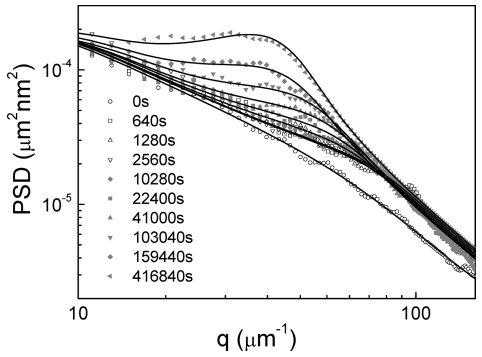

Figure 2. Power spectrum density (PSD) of a 3 nm thick PS (M_w = 115 kg/mol) film annealed at 110 °C. The legend shows the annealing times at which the PSDs were taken.

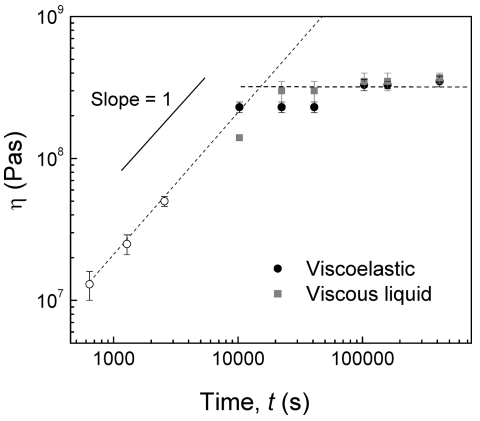

Figure 3. Fitted values of η obtained by model-fitting the PSDs shown in Figure 2 plotted versus time. The open (solid) symbols represent the values of η obtained by model-fitting the data in the rubbery plateau (terminal flow regime). The solid line is a line with slope = 1. The slanted dashed line is the best fit of the open symbols to the expression, $\eta = 2\mu_{plateau}t$. The horizontal dashed line shows the asymptotic value of η at long times.

for PS−SiO_x(100 nm)−Si films with h = 2 nm,[26] we find that $h^3q^2(\gamma q^2 + G'')/3 < 200$ Pa. As we will see below, our films have $\mu_{plateau} \approx 10$ kPa, which thus validates $(1 - \omega_{liq}\tau_r) > 0$.

By using the above estimates, one may find that the upper limit of $\omega_q\tau_r$, which also occurs at $q = q_c/\sqrt{2}$, is <1. By using eq 3, one may also find that the lower limit of $\omega_q\tau_r$ is −1 (see Figure 1). Together, the two give $|\omega_q| \leq 1/\tau_r$. The fact that $|\omega_q| \leq 1/\tau_r$ means that any capillary modes (which varies with time according to $\exp(-\omega_q t)$[20,21]) require a minimum duration of τ_r to relax or display a noticeable alteration in the amplitude. As a result, during the initial annealing where $t \ll \tau_r$, which is also when the film is in the elastic rubbery regime, the PSD remains stationary. Upon $t \gg \tau_r$, the film is in the viscous regime and the PSD evolves with $\omega \approx \omega_{liq}$ as discussed before. We examine the validity of these predictions for a representative set of time-sequenced PSDs shown in Figure 2, obtained from a 3 nm thick PS film with M_w = 115 kg/mol annealed at T = 110 °C. As one can see, the PSDs show no obvious alteration during the initial annealing from t = 640 to 2560 s as predicted by our model. It should be remarked that the apparent evolution from 0 to 640 s is attributable to the film undergoing the glass to rubber transition,[25] which is not accounted for by the Maxwell model used here. Beyond t = 2560 s, the PSD starts to evolve, suggesting that the film switched over to the terminal flow region around this time. The noted qualitative agreement between the model prediction and experiment shows that the simple dynamic behavior assumed here for $\eta(\omega)$ is adequate for describing the experimental observation. In the next section, we discuss how we analyzed the timed sequence of PSDs to determine the viscoelastic properties of the films.

■ RESULTS AND DISCUSSION

To perceive how the viscoelastic properties of the films may be deduced from the PSD in the elastic rubbery regime, we recall the approximated form of eq 1 reported before:[24]

$$A_q^2(t) = A_q^2(0)\Theta(q^* - q) + \frac{k_B T}{G''(h) + \gamma q^2 + \frac{3(\eta(\omega)/2t)}{h^3 q^2}} \quad (6)$$

In the above equatio, $\Theta(q^* - q)$ is the Heaviside step function and q^* is the wavevector whereat $\omega(q^*)t = 1$. The first term of eq 6 accounts for the low-q background of the PSD inherited from the initial surface structure of the film that has not been altered by the equilibration process.[24] Fredrickson et al.[34] had derived an expression for the PSD for purely elastic films. For elastic films with shear modulus equal to $\mu_{plateau}$, their result predicts that the equilibrium PSD is also given by eq 6 provided $\eta(\omega) = 2\mu_{plateau}t$.[25] Given this result, if we fit the PSDs in the elastic rubbery regime to eq 6 with η taken to be a constant fitting parameter, the fitted values of η should be proportional to t with the constant of proportionality being $2\mu_{plateau}$. The open symbols in Figure 3 represent the fitted values of η hence obtained from the PSDs, shown in Figure 2 and belong to the rubbery state (i.e., those with $t \leq$ 2560 s), plotted versus t. As seen, the result (open symbols) increases linearly with t as expected. The solid line in the same graph, with slope = 1, serves as a guide to the eye. From the data, we deduced that $\mu_{plateau} = 10 \pm 1$ kPa, which is similar to that found of the 125 nm thick films (see below). We remark that this is an order of magnitude smaller than the plateau modulus of the bulk polymer.[35] Polymer films displaying a plateau modulus smaller than the bulk value had been observed before[19,24] and ascribed to reduced interchain entanglement in the films that might result from spin-coating.[24] In spin-coating, a drop of the polymer solution is cast on the substrate, which is then spun at hundreds to thousands rpm, causing the solution to thin and dry within a minute. The short time over which the film dries is broadly believed to render the polymer chains insufficient time to attain the equilibrium conformation. Because the polymer is initially in the solution state, where individual chains are far apart with relatively little overlap, rapid drying can cause a conformation with fewer interchain entanglements than the equilibrium melt to be frozen in. Reduced entanglement was also reported in a recent experiment where the viscosity of as-cast PS films was measured.[16] It is noteworthy that reduced interchain entanglement is also expected in ultrathin films where the film thickness is smaller than the gyration radius of the polymer, as demonstrated in the crazing experiment by Si et al.[36] The fact that the plateau moduli of the 3 and 125 nm films were similar here may suggest that the same conformational or entanglement state was entrapped in these films at spin-coating. Alternatively, our observation may also be accounted for if intrachain entanglements are

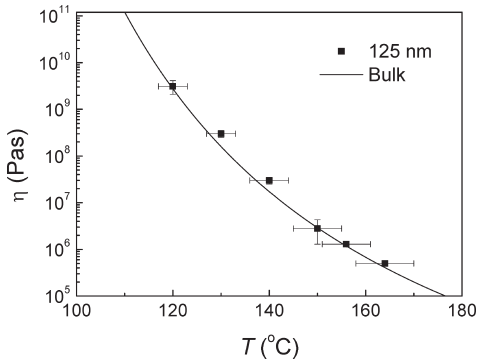

Figure 4. Plot of the long-time, steady-state viscosity, η_∞, versus the annealing temperature T for PS films with h = 125 nm and M_w = 212 kg/mol (solid squares). The solid line denotes the published viscosity of the bulk polymer.

also effective in affecting the rheological properties of the films (though we may expect them to be less effective than the interchain entanglements.) In analyzing the result from their crazing experiment, Si et al.[36] had assumed that the total entanglement density (i.e., the inter- plus intrachain entanglements) was a constant for different thicknesses and found good agreement with the experiment. It is thus possible that both the 3 and 125 nm as-cast films had been dominated by intrachain entanglements and so exhibit similar values for the plateau modulus.

Beyond $t = \tau_r$, the surface capillary modes begin to have sufficient time to relax, so the PSD can start to evolve. According to the present model, the evolution is governed by eq 1, with $\omega(q)$ given by eq 3. We thus fitted the PSDs in Figure 2 with $t > 2560$ s to eqs 1 and 3. In performing the fits, we treated η as the only fitting parameters and used either the experimental or literature values for the rest of the parameters. (For example, we used $\mu_{plateau}$ = 10 kPa as found above, T = 110 °C, h = 3 nm, and γ = 0.03 N/m, etc.) The result hence obtained is shown in Figure 3 by the black filled circles. As seen, the fitted values of η stabilize at about $(3 \pm 1) \times 10^8$ Pa s. It should, however, be mentioned that the majority of the films, especially those with thickness >10 nm, actually display a terminal viscosity that increases with time initially but saturates after a sufficiently long time. We denote the long-time saturated viscosity by η_∞ below. We have also used the liquid film model (namely, eq 1 and $\omega(q) = \omega_{liq}$) to fit the data, which are shown by the gray filled squares in Figure 3. As one can see, the result agrees with that obtained by using the viscoelastic film model within error bars—except for the first data point in the terminal flow regime measured at t = 10280 s, which clearly displays a smaller viscosity. This may be understood from the plots shown in Figure 1 that the relaxation rate $\omega(q)$ of the viscoelastic film model is bigger than that of the liquid film model ω_{liq} at short times, and only after long enough times do they converge. We have found good agreement between the two models to be common among the films we studied, suggesting that the liquid film model can be used to deduce the viscoelastic properties of the films with good approximation.

Next, we discuss the result we obtained when we measured thick PS films with h = 125 nm. Figure 4 displays the steady-state η_∞ found in these films plotted versus the annealing temperature, T. The solid line represents the published viscosity of bulk PS with the same M_w.[37] Previous studies[38−40] showed that thick films as such had the same T_g as the bulk polymer. The apparent good agreement between the steady-state viscosity of these films and the bulk viscosity therefore attests to our method for characterizing the dynamics of the films. The value of the plateau modulus found of these films was ∼12 kPa, which is also ∼10 times smaller than the bulk value and had been pointed out above. The fact that their steady-state viscosity η_∞ eventually acquired the bulk value at long times suggests that the films were able to recover the equilibrium entanglement conformation given sufficient annealing.

It is interesting to note that the published viscosity of bulk PS with M_w = 115 kg/mol at 110 °C (= 1.7×10^{10} Pa s)[37] is ∼2 orders of magnitude bigger than the counterpart steady-state effective viscosity, η_∞, found of the 3 nm film (Figure 3). We discuss whether the difference can be accounted for by reduced interchain entanglement in the 3 nm film. In a previous experiment,[39] we measured the thickness dependence, $T_g(h)$, of PS films on silicon with M_w = 13.7 and 550 kg/mol and found that $T_g(h)/T_g(\infty)$ was the same for the two M_w's. This suggests that reduced interchain entanglement is probably not a dominant factor for the T_g reduction and lowered effective η_∞ found in the 3 nm film. We believe that what is dominant is the surface mobile layer that had been experimentally found in both entangled[29,31] and unentangled PS films.[18,31] A recent experiment showed that a high-mobility surface layer could indeed cause the effective viscosity of unentangled PS films to decrease with decreasing film thickness.[18] Both preferential segregation of chain ends[31−33] and proximity of the chain segments[18,31] to the free surface have been attributed to be the origin of the surface mobile layer. On the basis that surface segregation of chain ends is stronger with lower M_w[32,33] and yet $T_g(h)/T_g(\infty)$ was found to be independent of the M_w,[39] we believe that the former is more important.

CONCLUSION

We have developed a method to measure the viscoelastic properties of entangled polymer films. Polystyrene films with molecular weights of 115 and 212 kg/mol and thicknesses of 3 and 125 nm, respectively, were used to demonstrate the method. The model utilized to analyze the data had been found to capture the viscoelastic behavior of the films quite well over the dynamic region including the rubbery plateau and terminal flow regimes. Our method allows the plateau shear modulus and zero-shear viscosity to be determined. We found that the plateau moduli of the films were an order of magnitude smaller than the bulk value, attributable to the as-cast films having a smaller density of entanglement than the bulk polymer. On the other hand, the steady-state viscosity of the 125 nm thick films was the same as the bulk, implying that the films were able to recover the equilibrium entanglement density when given long enough annealing.

AUTHOR INFORMATION

Corresponding Author

*E-mail: okctsui@bu.edu.

Present Addresses

†Center for Soft Condensed Matter Physics & Interdisciplinary Research, Soochow University, Suzhou 215123, P. R. China.

ACKNOWLEDGMENT

We thank Kari Dalnoki-Veress for illuminating discussions about inter- and intrachain entanglements in polymer films.

We are grateful to the support of the National Science Foundation through the projects DMR-0908651 and DMR-1004648.

REFERENCES

(1) Alcoutlabi, M.; McKenna, G. B. *J. Phys.: Condens. Matter* **2005**, *17*, R461–R524.
(2) Dalnoki-Veress, K.; Forrest, J. A.; Murray, C.; Gigault, C.; Dutcher, J. R. *Phys. Rev. E* **2001**, *62*, 5187–5200.
(3) Baschnagel, J.; Varnik, F. *J. Phys.: Condens. Matter* **2005**, *17*, R851–R953.
(4) Roth, C. B.; Dutcher, J. R. *J. Electroanal. Chem.* **2005**, *584*, 13–22.
(5) Tsui, O. K. C. *Polymer Thin Films*; World Scientific: Singapore, 2008; pp 267−294.
(6) Stoykovich, M. P.; Yoshimoto, K.; Nealey, P. F. *Appl. Phys. A: Mater. Sci. Process.* **2008**, *90*, 277–283.
(7) Fukao, K.; Miyamoto, Y. *Phys. Rev. E* **2000**, *61*, 1743–1754.
(8) Sharp, J. S.; Forrest, J. A. *Phys. Rev. E* **2003**, *67*, 031805.
(9) Fakhraai, Z.; Forrest, J. A. *Phys. Rev. Lett.* **2005**, *95*, 025701.
(10) Tsui, O. K. C.; Wang, X. P.; Ho, J. Y. L.; Ng, T. K.; Xiao, X. *Macromolecules* **2000**, *33*, 4198–4204.
(11) Wang, X. P.; Xiao, X.; Tsui, O. K. C. *Macromolecules* **2001**, *34*, 4180–4185.
(12) O'Connell, P. A.; McKenna, G. B. *Science* **2005**, *307*, 1760–1763.
(13) Masson, J.-L.; Green, P. F. *Phys. Rev. E* **2002**, *65*, 031806.
(14) Ding, Y.; Ro, H.; Douglas, J. F.; Okerberg, B. C.; Karim, A.; Soles, C. L. *ACS Nano* **2007**, *1*, 84–92.
(15) Akgun, B.; Ugur, G.; Jiang, Z.; Narayanan, S.; Song, S.; Lee, H.; Brittain, W. J.; Kim, H.; Sinha, S. K.; Foster, M. D. *Macromolecules* **2009**, *42*, 737–741.
(16) Barbero, D.; Steiner, U. *Phys. Rev. Lett.* **2009**, *102*, 248303.
(17) Yang, Z.; Lam, C.-H.; DiMasi, E.; Bouet, N.; Jordan-Sweet, J.; Tsui, O. K. C. *Appl. Phys. Lett.* **2009**, *94*, 251906.
(18) Yang, Z.; Fujii, Y.; Lee, F. K.; Lam, C.-H.; Tsui, O. K. C. *Science* **2010**, *328*, 1676–1679.
(19) Zhang, J.; Kim, H.; Jiao, X.; Lee, H.; Lee, Y.-J.; Byun, Y.; Song, S.; Eom, D.; Li, C.; Rafailovich, M. H. L., L. B.; Sinha, S. K. *Phys. Rev. Lett.* **2007**, *98*, 227801.
(20) Wang, Y. J.; Tsui, O. K. C. *Langmuir* **2006**, *22*, 1959–1963.
(21) Wang, Y. J.; Tsui, O. K. C. *J. Non-Cryst. Solids* **2006**, *352*, 4977–4982.
(22) Wang, Y. J.; Lam, C.-H.; Zhang, X.; Tsui, O. K. C. *Eur. Phys. J.: Spec. Top.* **2007**, *141*, 181–187.
(23) Tsui, O. K. C.; Wang, Y. J.; Zhao, H.; Du, B. *Eur. Phys. J. E* **2003**, *12*, 417–425.
(24) Tsui, O. K. C.; Wang, Y. J.; Lee, F. K.; Lam, C.-H.; Yang, Z. *Macromolecules* **2008**, *41*, 1465–1468.
(25) Yang, Z. H.; Wang, Y.; Todorova, L.; Tsui, O. K. C. *Macromolecules* **2008**, *41*, 8785–8788.
(26) Zhao, H.; Wang, Y. J.; Tsui, O. K. C. *Langmuir* **2005**, *21*, 5817–5824.
(27) Safran, S. A.; Klein, J. *J. Phys. (Paris)* **1993**, *3*, 749–757.
(28) Rubinstein, M.; Colby, R. H. *Polymer Physics*; Oxford University Press: New York, 2003.
(29) Fakhraai, Z.; Forrest, J. A. *Science* **2008**, *319*, 600–604.
(30) Wang, X. P.; Tsui, O. K. C.; Xiao, X. *Langmuir* **2002**, *18*, 7066–7072.
(31) Tanaka, K.; Takahara, A.; Kajiyama, T. *Macromolecules* **2000**, *33*, 7588–7593.
(32) Tanaka, K.; Taura, A.; Ge, S.-R.; Takahara, A.; Kajiyama, T. *Macromolecules* **1996**, *29*, 3040–3042.
(33) Tanaka, K.; Takahara, A.; Kajiyama, T. *Macromolecules* **1997**, *30*, 6626–6632.
(34) Fredrickson, G. H.; Ajdari, A.; Leibler, L.; Carton, J.-P. *Macromolecules* **1992**, *25*, 2882–2889.
(35) Strobl, G. R. *The Physics of Polymers*; Springer-Verlag: Berlin, 1996.
(36) Si, L.; Massa, M. V.; Dalnoki-Veress, K.; Brown, H. R.; Jones, R. A. L. *Phys. Rev. Lett.* **2005**, *94*, 127801.
(37) Majeste, J.-C.; Montfort, J.-P.; Allal, A.; Marin, G. *Rheol. Acta* **1998**, *37*, 486–499.
(38) Tsui, O. K. C.; Russell, T. P.; Hawker, C. *Macromolecules* **2001**, *34*, 5535–5539.
(39) Tsui, O. K. C.; Zhang, H. F. *Macromolecules* **2001**, *34*, 9139–9142.
(40) Clough, A.; Peng, D.; Yang, Z.; Tsui, O. K. C. *Macromolecules* **2011**, *44*, 1649–1653.